Electronic Supplementary Material (ESI) for Dalton Transactions.

Supporting Information

Terminal solvent effects on the anisotropy barriers of Dy_2 systems

Y. Jiang,[a] G. Brunet,[a] R. J. Holmberg, [a] F. Habib, [a] I. Korobkov, [a] and M. Murugesu*[a]

[a] *Department of Chemistry and Biomolecular Sciences, University of Ottawa, 10 Marie Curie, Ottawa, ON, Canada K1N 6N5. E-mail: m.murugesu@uottawa.ca; Tel: +1 (613) 562 5800 ext. 2733*

Table S1 Crystallographic data for dinuclear complexes **1–3.**

	1	**2**	**3**
formula	$C_{34}H_{36}Cl_2Dy_2N_8O_8$	$C_{34}H_{38}Cl_2Dy_2N_6O_8$	$C_{30}H_{33}Cl_2Dy_2N_6O_{10}$
fw	1080.61	1052.59	1033.52
T/K	200(2)	200(2)	200(2)
crystal system	Monoclinic	Monoclinic	Monoclinic
space group	$P2_1/n$	$P2_1/n$	$P2_1/c$
a/Å	9.2840(5)	9.2698(2)	9.4224(3)
b/Å	12.1401(6)	12.1313(3)	11.7141(4)
c/Å	17.5090(8)	16.9364(4)	30.8652(10)
α/deg	90	90	90
β/deg	98.4461(11)	101.2440(10)	96.162(2)
γ/deg	90	90	90
Vol/$Å^3$	1952.01(17)	1868.02(8)	3387.06(19)
Z	2	2	4
DC/ Mg m^{-3}	1.839	1.871	2.027
μ/mm^{-1}	3.994	4.170	4.602
Reflns collected	27137	11000	5747
GOF	1.017	1.093	1.244
*R1, wR*2 (>2σ(I))[a]	0.0267, 0.0648	0.0413, 0.0896	0.0897, 0.1836
*R1, wR*2 (all data)	0.0388, 0.0716	0.0319, 0.0853	0.1031, 0.1883

[a] $R=R_1=||F_o| - |F_c||/\Sigma|F_o|$; $wR_2 = \{[\Sigma w(F_o^2-F_c^2)^2]/[w(F_o^2)^2]\}^{1/2}$; $w=1/[\sigma^2(F_o^2)+(ap)^2+bp]$, where $p=[\max(F_o^2,0)+2Fc^2]/3$.

Table S2 Selected bond distances (Å) and angles (°) for complexes **1** and **2**.

	1	**2**
Dy1-Dy1a/Å	3.8937(3)	3.8538(3)
Dy1-O3/Å	2.337(2)	2.322(4)
Dy1-O3a/Å	2.316(2)	2.317(4)
Dy1-O4/Å	2.288(4)	2.381(3)
Dy1-Cl1/Å	2.613(1)	2.633(1)
Dy1-O3-Dy1a/°	113.60(9)	112.4(1)
O4-Dy1-Cl1/°	176.2(1)	163.41(9)

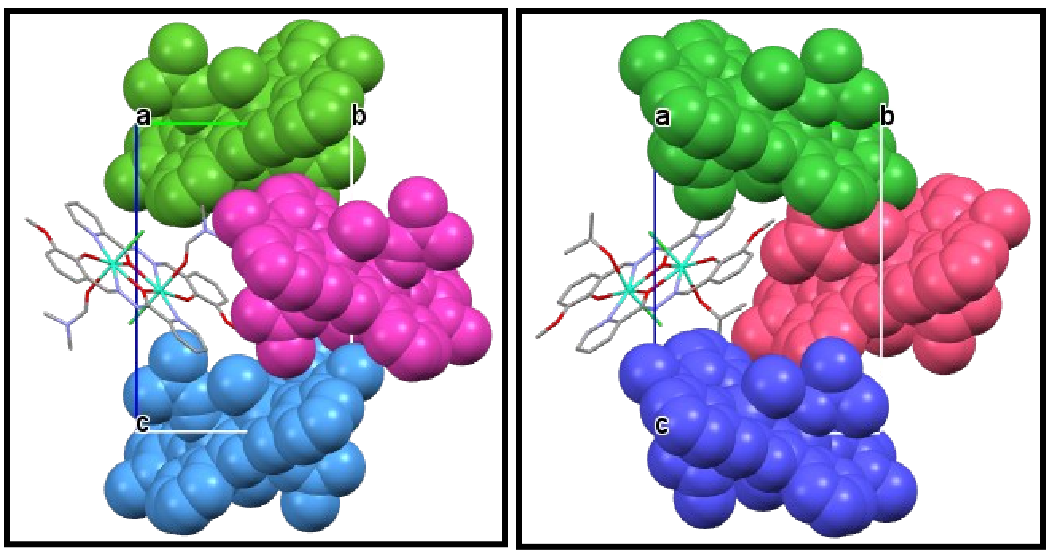

Fig. S1 Illustration of the packing arrangements of complexes **1** (left) and **2** (right). The shortest Dy-Dy distance for **1**: green-purple-9.42 Å, purple-blue-9.89 Å; for **4**: green-pink-9.31 Å, pink-blue-9.38 Å.

Table S3 Selected bond distances (Å) and angles (°) for complex **3**.

	3
Dy1-Dy2/Å	3.954(1)
Dy1-O3/Å	2.30(1)
Dy1-O6/Å	2.32(1)
Dy2-O3/Å	2.44(1)
Dy2-O6/Å	2.40(1)
Dy2-O10/Å	2.45(1)
Dy2-O7/Å	2.48(1)
Dy2-O8/Å	2.50(1)
Dy2-O9/Å	2.44(1)
Dy1-Cl1/Å	2.662(5)
Dy1-Cl2/Å	2.665(5)
C9-N2/Å	1.30(2)
C9-O3/Å	1.30(2)
C23-O6/Å	1.28(2)
C23-N5/Å	1.31(2)
Cl1-O9/Å	3.12(1)
Cl2-O10/Å	3.17(1)
Dy1-O3-Dy2/°	113.2(5)
Dy1-O6-Dy2/°	113.8(4)
Cl1-Dy1-Cl2/°	169.3(1)

Table S4 SHAPE constants of Dy_2 for complex **3**.

SHAPE code	Point group	Description	SHAPE constant
EP-9	D_{9h}	Enneagon	34.909
OPY-9	C_{8v}	Octagonal pyramid	23.177
HBPY-9	D_{7h}	Heptagonal bipyramid	18.619
JTC-9	C_{3v}	Johnson triangular cupola J3	13.944
JCCU-9	C_{4v}	Capped cube J8	10.742
CCU-9	C_{4v}	Spherical-relaxed capped cube	9.471
JCSAPR-9	C_{4v}	Capped square antiprism J10	2.002
CSAPR-9	C_{4v}	Spherical capped square antiprism	1.221
JTCTPR-9	D_{3h}	Tricapped trigonal prism J51	2.571
TCTPR-9	D_{3h}	Spherical tricapped trigonal prism	1.550
JTDIC-9	C_{3v}	Tridiminished icosahedron J63	12.072
HH-9	C_{2v}	Hula-hoop	9.515
MFF-9	C_s	Muffin	1.325

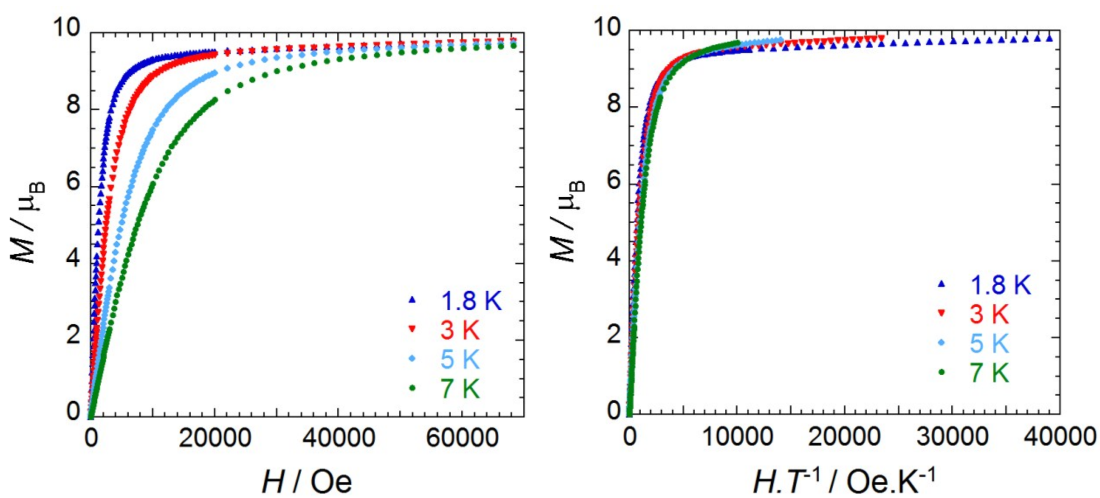

Fig. S2 Field dependence of the magnetization M at 1.8, 3, 5, and 7 K for complex **1** plotted as M *vs*. H (left) and M *vs*. HT^{-1} (right).

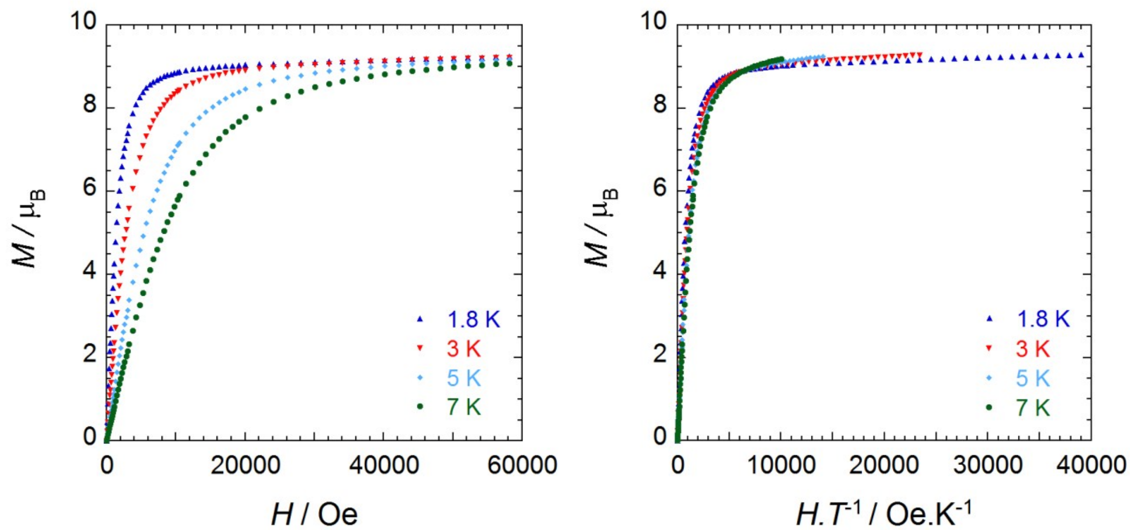

Fig S3 Field dependence of the magnetization M at 1.8, 3, 5, and 7 K for complex **2** plotted as M *vs*. H (left) and M *vs.* HT^{-1} (right).

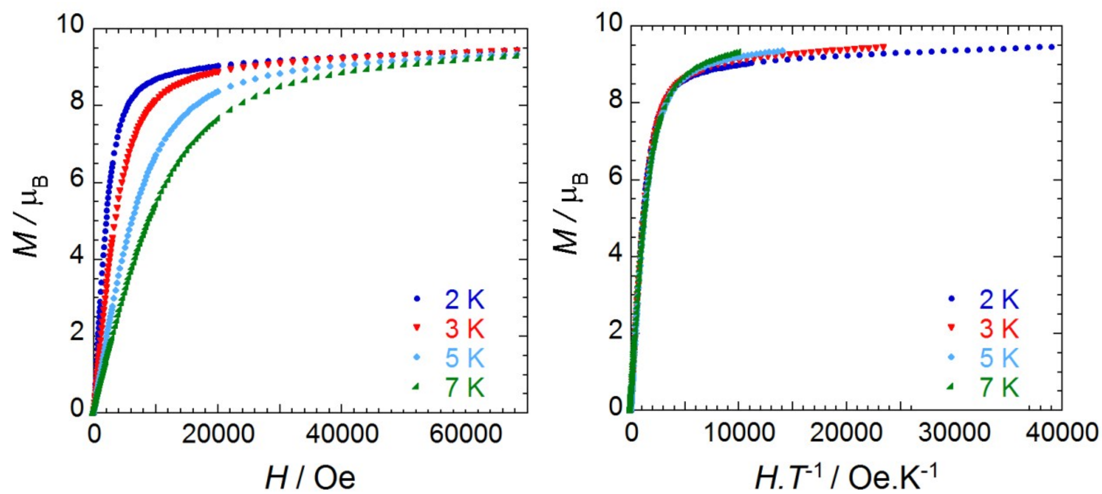

Fig S4 Field dependence of the magnetization M at 2, 3, 5, and 7 K for complex **3** plotted as M *vs*. H (left) and M *vs.* HT^{-1} (right).

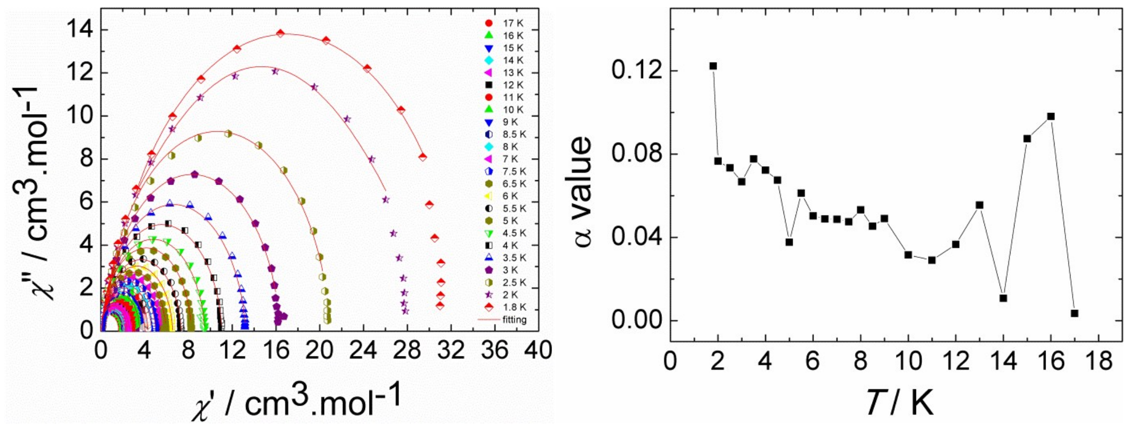

Fig. S5 Cole-Cole plot using the ac susceptibility data for complex **1** (left) and the obtained α values from the fit using a generalized Debye model plotted as α *vs.* T (right).

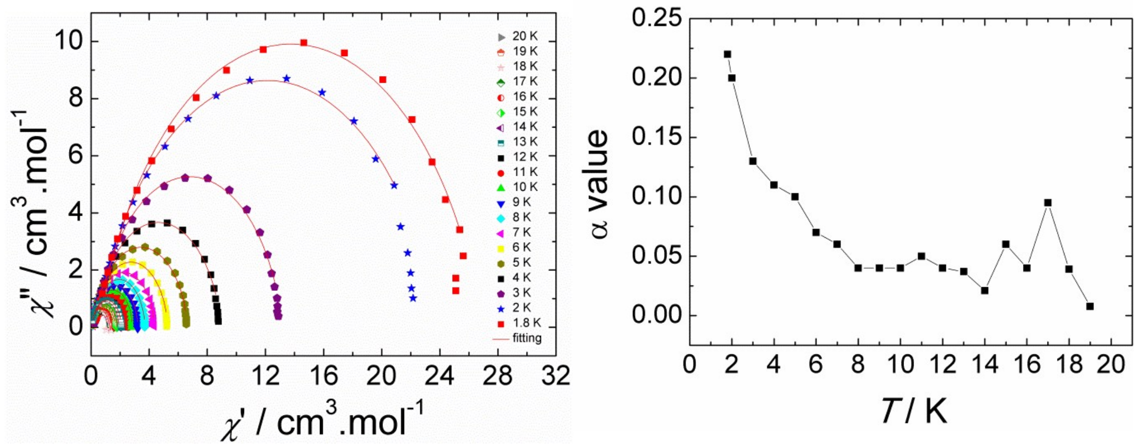

Fig. S6 Cole-Cole plot using the ac susceptibility data for complex **2** (left) and the obtained α values from the fit using a generalized Debye model plotted as α *vs.* T (right).